Acta Cryst E CRYSTALLOGRAPHIC COMMUNICATIONS

ISSN 2056-9890

Crystal structure and Hirshfeld surface analysis of 3-cyanophenylboronic acid

A. Jaquelin Cárdenas-Valenzuela,[a] Gerardo González-García,[b] Ramón Zárraga-Nuñez,[b] Herbert Höpfl,[c] José J. Campos-Gaxiola[a] and Adriana Cruz-Enríquez[a]*

[a]Facultad de Ingeniería Mochis, Universidad Autónoma de Sinaloa, Fuente de Poseidón y Prol. A. Flores S/N, CP 81223, C.U. Los Mochis, Sinaloa, México, [b]Departamento de Química, División de Ciencias Naturales y Exactas, Campus Guanajuato, Universidad de Guanajuato, Sede Noria Alta, Noria Alta S/N, Col. Noria Alta, CP 36050, Guanajuato, Gto., México, and [c]Centro de Investigaciones Químicas, Instituto de Investigación en Ciencias Básicas y Aplicadas, Universidad Autónoma del Estado de Morelos, Av. Universidad 1001, CP 62209, Cuernavaca, Morelos, México. *Correspondence e-mail: cruzadriana@uas.edu.mx

Received 12 February 2018
Accepted 23 February 2018

Edited by H. Stoeckli-Evans, University of Neuchâtel, Switzerland

Keywords: crystal structure; boronic acid; hydrogen bonding; offset π–π interactions; Hirshfeld surface analysis.

CCDC reference: 1825335

Supporting information: this article has supporting information at journals.iucr.org/e

In the title compound, $C_7H_6BNO_2$, the mean plane of the –$B(OH)_2$ group is twisted by 21.28 (6)° relative to the cyanophenyl ring mean plane. In the crystal, molecules are linked by O—H···O and O—H···N hydrogen bonds, forming chains propagating along the [101] direction. Offset π–π and B···π stacking interactions link the chains, forming a three-dimensional network. Hirshfeld surface analysis shows that van der Waals interactions constitute a further major contribution to the intermolecular interactions, with H···H contacts accounting for 25.8% of the surface.

1. Chemical context

Boron-containing compounds and particularly arylboronic acid are an important class of compounds in the fields of organic and medicinal chemistry, and have played a role in the development of modern organic synthesis, macromolecular chemistry, crystal engineering and molecular recognition (Fujita *et al.*, 2008; Severin, 2009). As a result of their peculiar dynamic covalent reactivity with alcohols (Jin *et al.*, 2013), arylboronic acids and their dehydrated derivatives enable the self-assembly of a large variety of architectures resulting from boronate esterification (Takahagi *et al.* 2009) as well as boroxine (Côté *et al.*, 2005) and spiroborate formation (Du *et al.*, 2016).

Boronic acids form neutral and charge-assisted homo- and heterodimeric hydrogen-bonding patterns resembling characteristics similar to those found for carboxylic acids (see Fig. 1*a*). However, the –$B(OH)_2$ moiety contains two O—H

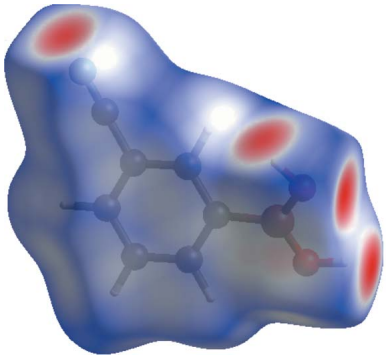

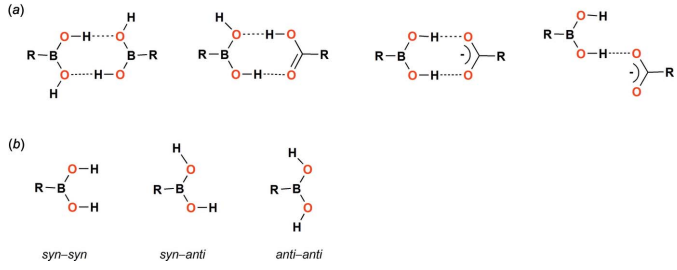

Figure 1
(*a*) Neutral and charge-assisted homo- and heterodimeric hydrogen-bonding motifs involving boronic acids. (*b*) Conformations of the boronic acid moiety.

hydrogen-bond donors and can, thus, form two O—H···*X* hydrogen bonds and adopt different conformations (see Fig. 1*b*). This enables the generation of hydrogen-bonding networks with increased dimensionality (one to three dimensions) in the solid state (Fournier *et al.*, 2003; Madura *et al.*, 2015; Georgiou *et al.*, 2017). In recent years, boronic acids have also been explored in the context of forming multicomponent molecular complexes with organic carboxylic acids (–COOH), amides (–$CONH_2$), alcohols (–OH) and pyridines, which are based on molecular recognition processes (Rodríguez-Cuamatzi *et al.*, 2005; Madura *et al.*, 2014; Hernández-Paredes *et al.*, 2015; Campos-Gaxiola *et al.*, 2017; Pedireddi & Lekshmi, 2004; Vega *et al.*, 2010; TalwelkarShimpi *et al.*, 2016). As part of our ongoing studies in this area, we report herein on the molecular and crystal structures of 3-cyanophenylboronic acid, I. In addition, a Hirshfeld surface analysis was performed to visualize and quantify the intermolecular interactions in the crystal structure of compound (I).

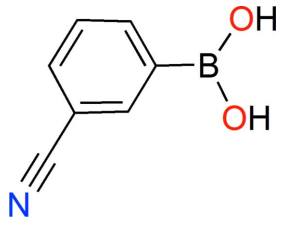

2. Structural commentary

The molecular structure of the title compound (I) is illustrated in Fig. 2. It can be seen that the –$B(OH)_2$ group adopts the most preferred *syn–anti* conformation (Lekshmi & Pedireddi, 2007). As a result of the H···H repulsion between the *endo*-oriented B—OH hydrogen and the C—H hydrogen in position 2 of the aromatic ring, the –$B(OH)_2$ mean plane is twisted by 21.28 (6)° relative to the cyanophenyl ring mean plane. This torsion disables intramolecular C—H···O hydrogen bonding between the oxygen atom of the *exo*-oriented B—OH function and weakens the B—C π–π bonding interactions (Durka *et al.*, 2012). The B1—O1, B1—O2 and B1—C1 bond lengths are 1.3455 (17), 1.3661 (18) and 1.5747 (18) Å, respectively. For comparison, in coplanar triphenyl boroxine the B—C bond lengths range from 1.544 (4) to 1.549 (4) Å (Brock *et al.*, 1987). The C≡N bond length of 1.1416 (18) Å is typical for a bond with triple-bond character.

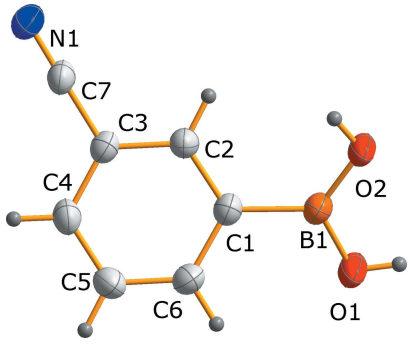

Figure 2
The molecular structure of the title compound (I), with the atom labeling. Displacement ellipsoids are drawn at the 50% probability level.

Table 1
Hydrogen-bond geometry (Å, °).

D—H···*A*	*D*—H	H···*A*	*D*···*A*	*D*—H···*A*
O1—H1···O2^{i}	0.82	1.98	2.796 (1)	170
O2—H2···N1^{ii}	0.82	2.12	2.909 (2)	160
C2—H2*A*···N1^{ii}	0.93	2.71	3.452 (2)	138
C4—H4···O1^{iii}	0.93	2.67	3.469 (2)	144

Symmetry codes: (i) $-x+2, -y+1, -z+1$; (ii) $-x+1, -y+1, -z$; (iii) $x-1, -y+\frac{3}{2}, z-\frac{1}{2}$.

3. Supramolecular features

In the crystal of (I), the boronic acid molecules are in the first instance associated to form chains through two well-known double-bridged homodimeric motifs based on a –BOH···O(H)B– [motif **A**; graph set $R_2^2(8)$] and C—H···N≡C hydrogen bonds [motif **B**; graph set $R_2^2(10)$]. This hydrogen-bonding pattern is strengthened further by a –BOH···N≡C contact [motif **C**; graph set $R_2^1(7)$] (Fig. 3*a*, Table 1). In comparison to the crystal structure of 4-cyanophenylboronic acid, where the chains are almost linear (TalwelkarShimpi *et al.*, 2017), in (I) they have a pronounced zigzag topology. The O1···O2^{i}, C2···N1^{ii} and O2···N1^{ii} separations in motifs **A**, **B** and **C** are 2.796 (1), 3.452 (2) and 2.909 (2) Å, respectively (Table 1), and are similar to distances reported for related systems (Rodríguez-Cuamatzi *et al.*, 2005; TalwelkarShimpi *et al.*, 2017). Within the crystal structure,

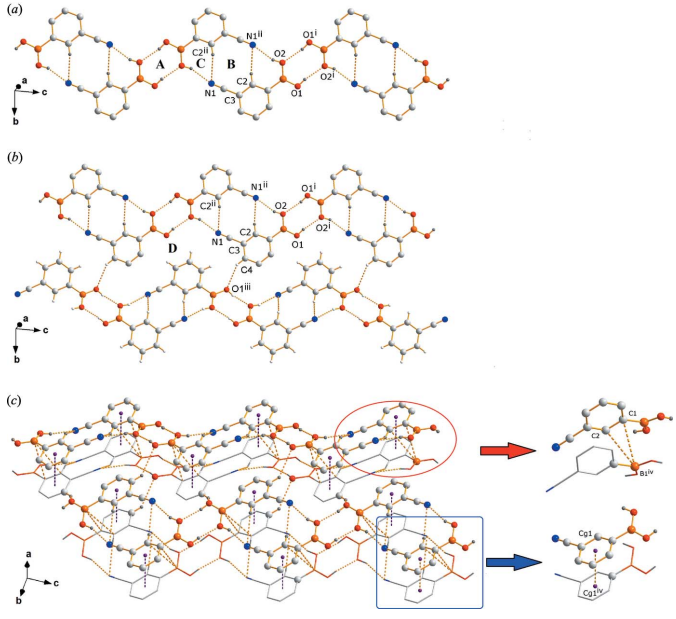

Figure 3
Hydrogen-bonding motifs and π–π interactions found in the crystal structure of (I). [Symmetry codes: (i) $2-x, 1-y, 1-z$; (ii) $1-x, 1-y, -z$; (iii) $-1+x, \frac{3}{2}-y, -\frac{1}{2}+z$; (iv) $-1+x, y, z$.]

neighboring tapes are linked through additional C—H···O contacts to give an overall two-dimensional network running parallel to ($\bar{1}$01) with macrocyclic motifs **D** [graph set $R_6^6(26)$], see Fig. 3*b*. The C4···O1^{iii} distance is 3.469 (2) Å, see Table 1. The resulting 2D networks stack in a parallel fashion to form a layered 3D structure based on offset π–π interactions between adjacent 3-cyanophenylboronic acid molecules [Cg···Cg^{iv} = 3.8064 (8) Å; slippage 1.38 Å; symmetry code (iv) = $-1+x, y, z$] and η^2-type B···π contacts with B···C distances of 3.595 (2) and 3.673 (2) Å (Fig. 3*c*). Similar interactions are also depicted in molecular crystals formed between 1,4-benzenediboronic acid and aromatic amine *N*-oxides (Sarma & Baruah, 2009; Sarma *et al.*, 2011).

4. Hirshfeld surface analysis

Hirshfeld surfaces and fingerprint plots were generated for (I) based on the crystallographic information file (CIF) using *CrystalExplorer* (Hirshfeld, 1977; McKinnon *et al.*, 2004). Hirshfeld surfaces enable the visualization of intermolecular interactions by different colors and color intensity, representing short or long contacts and indicating the relative strength of the interactions. Fig. 4 shows the Hirshfeld surface of the title compound mapped over d_{norm} (−0.60 to 0.90 Å) and the shape-index (−1.0 to 1.0 Å). In the d_{norm} map, the vivid red spots in the Hirshfeld surface are due to short normalized O···H and N···H distances corresponding to O—H···O and O—H···N interactions. The white spots represent the contacts resulting from C—H···N hydrogen bonding (Fig. 4*a*). On the shape-index surface for compound (I), convex blue regions represent hydrogen-donor groups and concave red regions represent hydrogen-acceptor groups. The –B(OH)$_2$ group behaves simultaneously as a donor and an acceptor, meanwhile the –C≡N group is an acceptor only. The occurrence of offset π–π interactions is indicated by adjacent red and blue triangles (Fig. 4*b*).

The two-dimensional fingerprint plots quantify the contributions of each type of non-covalent interaction to the Hirshfeld surface (McKinnon *et al.*, 2007). The major contribution with 25.8% of the surface is due to H···H contacts, which represent van der Waals interactions, followed by N···H and O···H interactions, which contribute 23.6 and 20.4%, respectively (these contributions are observed as two sharp peaks in the plot of Fig. 5). This behavior is usual for strong hydrogen bonds (Spackman & McKinnon, 2002). Finally, the presence of C···C (11.4%) and B···C (2.3%) contacts corresponds to the π–π and B···π interactions, respectively, established in the crystal structure analysis section.

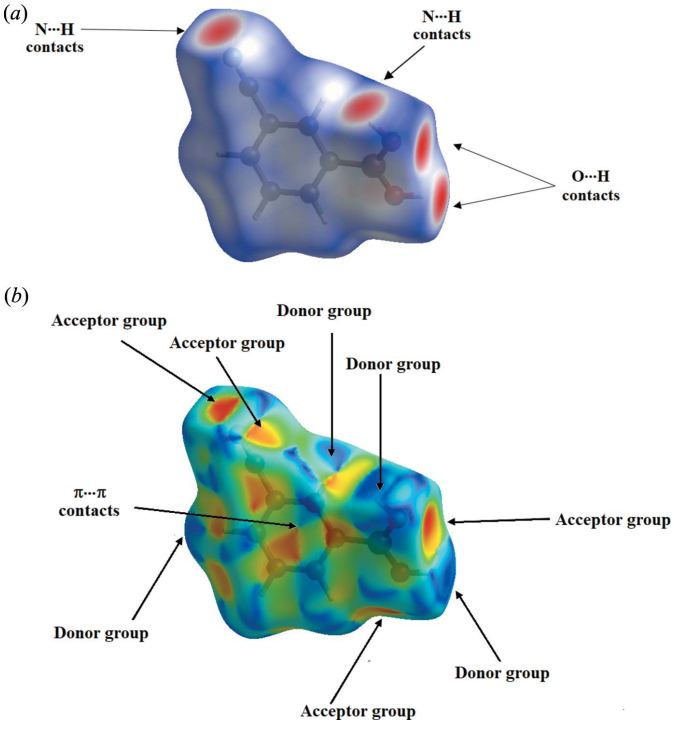

Figure 4
Hirshfeld surfaces for compound (I), mapped with d_{norm} (top) and shape-index (bottom).

5. Experimental

3-Cyanophenylboronic acid and the solvent used in this work are commercially available and were used without further purification. For single-crystal growth, a solution of 3-cyanophenylboronic acid (0.050 g) in 5 ml of ethanol was heated to reflux for 15 min. The solution was left to evaporate slowly at room temperature, giving after one week colorless crystals suitable for single-crystal X-ray diffraction analysis.

6. Refinement

Crystal data, data collection and structure refinement details are summarized in Table 2. Hydrogen atoms were positioned geometrically (O—H = 0.82 Å and C—H = 0.93 Å) and refined using a riding model, with U_{iso}(H) = 1.2U_{eq}(C) and 1.5U_{eq}(O).

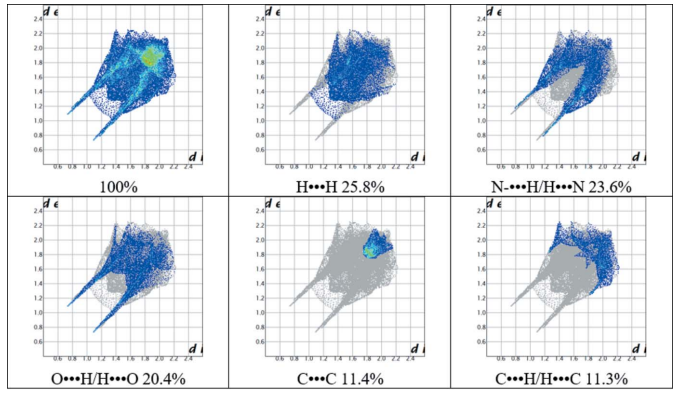

Figure 5
Two-dimensional fingerprints of compound (I), showing H···H, N···H, O···H, C···C and C···H close contacts.

Funding information

This work was supported financially by the Consejo Nacional de Ciencia y Tecnología (CONACYT, Project Nos. 177616 and 229929) and Red Temática de Química Supramolecular (CONACYT, Project No. 281251). AJCV thanks the Consejo Nacional de Ciencia y Tecnología (CONACYT) for a graduate scholarship (273977).

References

Brock, C. P., Minton, R. P. & Niedenzu, K. (1987). *Acta Cryst.* C**43**, 1775–1779.

Campos-Gaxiola, J. J., García-Grajeda, B. A., Hernández-Ahuactzi, I. F., Guerrero-Álvarez, J. A., Höpfl, H. & Cruz-Enríquez, A. (2017). *CrystEngComm*, **19**, 3760–3775.

Côté, A. P., Benin, A. I., Ockwig, N. W., O'Keeffe, M., Matzger, A. J. & Yaghi, O. M. (2005). *Science*, **310**, 1166–1170.

Dolomanov, O. V., Bourhis, L. J., Gildea, R. J., Howard, J. A. K. & Puschmann, H. (2009). *J. Appl. Cryst.* **42**, 339–341.

Du, Y., Yang, H., Whiteley, J. M., Wan, S., Jin, Y., Lee, S. H. & Zhang, W. (2016). *Angew. Chem. Int. Ed.* **55**, 1737–1741.

Durka, K., Jarzembska, K. N., Kamiński, R., Luliński, S., Serwatowski, J. & Woźniak, K. (2012). *Cryst. Growth Des.* **12**, 3720–3734.

Fournier, J. H., Maris, T., Wuest, J. D., Guo, W. & Galoppini, E. (2003). *J. Am. Chem. Soc.* **125**, 1002–1006.

Fujita, N., Shinkai, S. & James, T. D. (2008). *Chem. Asian J.* **3**, 1076–1091.

Georgiou, I., Kervyn, S., Rossignon, A., De Leo, F., Wouters, J., Bruylants, G. & Bonifazi, D. (2017). *J. Am. Chem. Soc.* **139**, 2710–2727.

Hernández-Paredes, J., Olvera-Tapia, A. L., Arenas-García, J. I., Höpfl, H., Morales-Rojas, H., Herrera-Ruiz, D., Gonzaga-Morales, A. I. & Rodríguez-Fragoso, L. (2015). *CrystEngComm*, **17**, 5166–5186.

Hirshfeld, F. L. (1977). *Theor. Chim. Acta*, **44**, 129–138.

Jin, Y., Yu, C., Denman, R. J. & Zhang, W. (2013). *Chem. Soc. Rev.* **42**, 6634–6654.

Lekshmi, N. S. & Pedireddi, V. R. (2007). *Cryst. Growth Des.* **7**, 944–949.

Madura, I. D., Adamczyk-Woźniak, A. & Sporzyński, A. (2015). *J. Mol. Struct.* **1083**, 204–211.

Madura, I. D., Czerwińska, K. & Sołdańska, D. (2014). *Cryst. Growth Des.* **14**, 5912–5921.

McKinnon, J. J., Jayatilaka, D. & Spackman, M. A. (2007). *Chem. Commun.* pp. 3814–3816.

McKinnon, J. J., Spackman, M. A. & Mitchell, A. S. (2004). *Acta Cryst.* B**60**, 627–668.

Palatinus, L. & Chapuis, G. (2007). *J. Appl. Cryst.* **40**, 786–790.

Palatinus, L., Prathapa, S. J. & van Smaalen, S. (2012). *J. Appl. Cryst.* **45**, 575–580.

Palatinus, L. & van der Lee, A. (2008). *J. Appl. Cryst.* **41**, 975–984.

Table 2
Experimental details.

Crystal data	
Chemical formula	$C_7H_6BNO_2$
M_r	146.94
Crystal system, space group	Monoclinic, $P2_1/c$
Temperature (K)	293
a, b, c (Å)	3.8064 (2), 16.156 (1), 11.4585 (4)
β (°)	93.472 (4)
V (Å^3)	703.36 (6)
Z	4
Radiation type	Mo $K\alpha$
μ (mm^{-1})	0.10
Crystal size (mm)	0.48 × 0.25 × 0.20
Data collection	
Diffractometer	Rigaku OD SuperNova Single source at offset EosS2
Absorption correction	Gaussian (*CrysAlis PRO*; Rigaku OD, 2015)
T_{min}, T_{max}	0.992, 0.996
No. of measured, independent and observed [$I > 2\sigma(I)$] reflections	7332, 1434, 1347
R_{int}	0.023
(sin $\theta/\lambda)_{max}$ (Å^{-1})	0.625
Refinement	
$R[F^2 > 2\sigma(F^2)]$, $wR(F^2)$, S	0.042, 0.110, 1.09
No. of reflections	1434
No. of parameters	102
H-atom treatment	H-atom parameters constrained
$\Delta\rho_{max}$, $\Delta\rho_{min}$ (e Å^{-3})	0.20, −0.24

Computer programs: *CrysAlis PRO* (Rigaku OD, 2015), *SUPERFLIP* (Palatinus & Chapuis, 2007; Palatinus & van der Lee, 2008; Palatinus *et al.*, 2012), *SHELXL2016* (Sheldrick, 2015) and *OLEX2* (Dolomanov *et al.*, 2009).

Pedireddi, V. R. & Lekshmi, N. S. (2004). *Tetrahedron Lett.* **45**, 1903–1906.

Rigaku OD (2015). *CrysAlis PRO*. Rigaku Oxford Diffraction. Yarnton, England.

Rodríguez-Cuamatzi, P., Arillo-Flores, O. I., Bernal-Uruchurtu, M. I. & Höpfl, H. (2005). *Cryst. Growth Des.* **5**, 167–175.

Sarma, R. & Baruah, J. B. (2009). *J. Mol. Struct.* **920**, 350–354.

Sarma, R., Bhattacharyya, P. K. & Baruah, J. B. (2011). *Comput. Theor. Chem.* **963**, 141–147.

Severin, K. (2009). *Dalton Trans.* pp. 5254–5264.

Sheldrick, G. M. (2015). *Acta Cryst.* C**71**, 3–8.

Spackman, M. A. & McKinnon, J. J. (2002). *CrystEngComm*, **4**, 378–392.

Takahagi, H., Fujibe, S. & Iwasawa, N. (2009). *Chem. Eur. J.* **15**, 13327–13330.

TalwelkarShimpi, M., Öberg, S., Giri, L. & Pedireddi, V. R. (2016). *RSC Adv.* **6**, 43060–43068.

TalwelkarShimpi, M., Öberg, S., Giri, L. & Pedireddi, V. R. (2017). *Cryst. Growth Des.* **17**, 6247–6254.

Vega, A., Zarate, M., Tlahuext, H. & Höpfl, H. (2010). *Acta Cryst.* C**66**, o219–o221.

supporting information

Acta Cryst. (2018). E**74**, 441-444 [https://doi.org/10.1107/S2056989018003146]

Crystal structure and Hirshfeld surface analysis of 3-cyanophenylboronic acid

A. Jaquelin Cárdenas-Valenzuela, Gerardo González-García, Ramón Zárraga- Nuñez, Herbert Höpfl, José J. Campos-Gaxiola and Adriana Cruz-Enríquez

Computing details

Data collection: *CrysAlis PRO* (Rigaku OD, 2015); cell refinement: *CrysAlis PRO* (Rigaku OD, 2015); data reduction: *CrysAlis PRO* (Rigaku OD, 2015); program(s) used to solve structure: SUPERFLIP (Palatinus & Chapuis, 2007; Palatinus & van der Lee, 2008; Palatinus *et al.*, 2012); program(s) used to refine structure: *SHELXL2016* (Sheldrick, 2015); molecular graphics: *OLEX2* (Dolomanov *et al.*, 2009); software used to prepare material for publication: *OLEX2* (Dolomanov *et al.*, 2009).

3-Cyanophenylboronic acid

Crystal data

$C_7H_6BNO_2$
M_r = 146.94
Monoclinic, $P2_1/c$
a = 3.8064 (2) Å
b = 16.156 (1) Å
c = 11.4585 (4) Å
β = 93.472 (4)°
V = 703.36 (6) Å^3
Z = 4
$F(000)$ = 304
D_x = 1.388 Mg m^{-3}
Mo $K\alpha$ radiation, λ = 0.71073 Å
Cell parameters from 4312 reflections
θ = 4.4–29.1°
μ = 0.10 mm^{-1}
T = 293 K
Block, colourless
0.48 × 0.25 × 0.20 mm

Data collection

Rigaku OD SuperNova Single source at offset EosS2 diffractometer
Radiation source: micro-focus sealed X-ray tube, SuperNova (Mo) X-ray Source
Mirror monochromator
Detector resolution: 8.0945 pixels mm^{-1}
ω scans
Absorption correction: gaussian (CrysAlis PRO; Rigaku OD, 2015)
T_{min} = 0.992, T_{max} = 0.996
7332 measured reflections
1434 independent reflections
1347 reflections with $I > 2\sigma(I)$
R_{int} = 0.023
θ_{max} = 26.4°, θ_{min} = 3.6°
h = −4→4
k = −20→20
l = −14→14

Refinement

Refinement on F^2
Least-squares matrix: full
$R[F^2 > 2\sigma(F^2)]$ = 0.042
$wR(F^2)$ = 0.110
S = 1.09
1434 reflections
102 parameters
0 restraints
Primary atom site location: iterative
Secondary atom site location: difference Fourier map
Hydrogen site location: inferred from neighbouring sites
H-atom parameters constrained

$w = 1/[\sigma^2(F_o^2) + (0.0566P)^2 + 0.1839P]$
where $P = (F_o^2 + 2F_c^2)/3$
$(\Delta/\sigma)_{max} < 0.001$

$\Delta\rho_{max} = 0.20$ e Å^{-3}
$\Delta\rho_{min} = -0.24$ e Å^{-3}

Special details

Geometry. All esds (except the esd in the dihedral angle between two l.s. planes) are estimated using the full covariance matrix. The cell esds are taken into account individually in the estimation of esds in distances, angles and torsion angles; correlations between esds in cell parameters are only used when they are defined by crystal symmetry. An approximate (isotropic) treatment of cell esds is used for estimating esds involving l.s. planes.

Fractional atomic coordinates and isotropic or equivalent isotropic displacement parameters (Å²)

	x	*y*	*z*	U_{iso}*/U_{eq}
O2	0.8906 (3)	0.49351 (6)	0.34935 (8)	0.0436 (3)
H2	0.881271	0.482459	0.279381	0.065*
O1	0.8143 (3)	0.60701 (6)	0.47187 (8)	0.0507 (3)
H1	0.900315	0.572989	0.518407	0.076*
N1	0.0762 (4)	0.58588 (8)	−0.12243 (11)	0.0485 (4)
C3	0.3424 (3)	0.65006 (8)	0.06942 (10)	0.0307 (3)
C7	0.1909 (4)	0.61462 (8)	−0.03743 (11)	0.0355 (3)
C1	0.6246 (3)	0.62961 (8)	0.26214 (10)	0.0302 (3)
C2	0.4765 (3)	0.59744 (8)	0.15775 (11)	0.0309 (3)
H2A	0.467006	0.540428	0.146805	0.037*
C4	0.3561 (4)	0.73542 (8)	0.08286 (12)	0.0367 (3)
H4	0.267843	0.770116	0.023320	0.044*
C6	0.6325 (4)	0.71575 (8)	0.27423 (11)	0.0352 (3)
H6	0.727616	0.738593	0.343630	0.042*
C5	0.5031 (4)	0.76802 (8)	0.18615 (12)	0.0400 (3)
H5	0.515094	0.825073	0.196425	0.048*
B1	0.7827 (4)	0.57324 (9)	0.36442 (12)	0.0336 (3)

Atomic displacement parameters (Å²)

	U^{11}	U^{22}	U^{33}	U^{12}	U^{13}	U^{23}
O2	0.0679 (7)	0.0371 (5)	0.0242 (5)	0.0103 (5)	−0.0092 (5)	−0.0004 (4)
O1	0.0810 (8)	0.0414 (6)	0.0278 (5)	0.0165 (5)	−0.0120 (5)	−0.0029 (4)
N1	0.0625 (9)	0.0474 (7)	0.0339 (7)	0.0077 (6)	−0.0115 (6)	−0.0044 (5)
C3	0.0303 (6)	0.0361 (7)	0.0254 (6)	0.0025 (5)	−0.0001 (5)	0.0001 (5)
C7	0.0398 (7)	0.0365 (7)	0.0295 (7)	0.0077 (5)	−0.0031 (5)	0.0028 (5)
C1	0.0304 (6)	0.0332 (7)	0.0267 (6)	0.0014 (5)	−0.0002 (5)	0.0017 (5)
C2	0.0343 (7)	0.0291 (6)	0.0290 (6)	0.0019 (5)	−0.0011 (5)	0.0005 (5)
C4	0.0426 (8)	0.0353 (7)	0.0320 (7)	0.0063 (5)	0.0004 (5)	0.0067 (5)
C6	0.0397 (7)	0.0358 (7)	0.0296 (6)	−0.0019 (5)	−0.0016 (5)	−0.0031 (5)
C5	0.0520 (8)	0.0287 (7)	0.0390 (8)	0.0007 (6)	0.0009 (6)	0.0001 (5)
B1	0.0385 (8)	0.0347 (8)	0.0268 (7)	0.0006 (6)	−0.0038 (6)	0.0010 (5)

Geometric parameters (Å, º)

O2—B1	1.3661 (18)	C1—C2	1.3917 (17)
O1—B1	1.3455 (17)	C1—C6	1.3987 (18)
N1—C7	1.1416 (18)	C1—B1	1.5747 (18)
C3—C7	1.4401 (18)	C4—C5	1.3825 (19)
C3—C2	1.3948 (17)	C6—C5	1.3834 (19)
C3—C4	1.3882 (19)		
C2—C3—C7	119.00 (12)	C1—C2—C3	120.50 (12)
C4—C3—C7	119.98 (11)	C5—C4—C3	118.95 (12)
C4—C3—C2	121.02 (12)	C5—C6—C1	122.04 (12)
N1—C7—C3	178.81 (15)	C4—C5—C6	119.98 (12)
C2—C1—C6	117.51 (11)	O2—B1—C1	123.75 (11)
C2—C1—B1	122.70 (11)	O1—B1—O2	119.15 (12)
C6—C1—B1	119.79 (11)	O1—B1—C1	117.10 (12)
C3—C4—C5—C6	−0.2 (2)	C2—C1—B1—O1	−159.37 (13)
C7—C3—C2—C1	−179.96 (12)	C4—C3—C2—C1	0.64 (19)
C7—C3—C4—C5	−179.92 (12)	C6—C1—C2—C3	0.00 (18)
C1—C6—C5—C4	0.9 (2)	C6—C1—B1—O2	−158.17 (13)
C2—C3—C4—C5	−0.5 (2)	C6—C1—B1—O1	21.14 (19)
C2—C1—C6—C5	−0.8 (2)	B1—C1—C2—C3	−179.50 (12)
C2—C1—B1—O2	21.3 (2)	B1—C1—C6—C5	178.76 (13)

Hydrogen-bond geometry (Å, º)

D—H···*A*	*D*—H	H···*A*	*D*···*A*	*D*—H···*A*
O1—H1···O2^{i}	0.82	1.98	2.796 (1)	170
O2—H2···N1^{ii}	0.82	2.12	2.909 (2)	160
C2—H2*A*···N1^{ii}	0.93	2.71	3.452 (2)	138
C4—H4···O1^{iii}	0.93	2.67	3.469 (2)	144

Symmetry codes: (i) −*x*+2, −*y*+1, −*z*+1; (ii) −*x*+1, −*y*+1, −*z*; (iii) *x*−1, −*y*+3/2, *z*−1/2.